FLOOD INUNDATION EXTRACTION BASED ON DECISION-LEVEL DATA FUSION: A CASE IN PERU

M. Shen[1,2], F. Zhang[1,2,*], C.Y. Wu[1,2]

[1]School of Earth Sciences, Zhejiang University, Hangzhou 310028, China - shenm@zju.edu.cn; zfcarnation@zju.edu.cn; wuchuyi@zju.edu.cn
[2]Zhejiang Provincial Key Laboratory of Geographic Information Science, Hangzhou 310028, China

KEY WORDS: flood, flood inundation extraction, deep learning, decision-level data fusion

ABSTRACT:

Every year, millions of people affected and huge property losses by floods were recorded in many parts of the world. Accurately flood inundated areas extraction is essential for disaster reduction. Existed studies have used multi-spectral (MS) data and synthetic-aperture radar (SAR) data or the fusion data to extract flood inundated areas. However, most data fusion methods think less about regional difference and the complementarities between different models. This study explores a new decision-level data fusion method, which pays more attention to the complementarities between models. First, we construct models trained by diverse bands of Sentinel-1/2 and water indices. Then, divide the whole study area into three parts, cloud-free & non-water area, cloud-free & flood area and cloud area, and select the models suitable for the three areas. Third, combine water extents extracted by selected models with decision tree to obtain water extents before and after disaster. Finally, subtract the water extent before disaster from the water extent after disaster to get flood inundated areas. The experiments in Peru indicated that our method increases the Intersection over Union (IoU) of water extraction to 0.69. Moreover, our method successfully reduces the impact of cloud and shadow owing to the fusion of different features.

1. INTRODUCTION

Flood is one of the most common meteorological disasters, which occurs rapidly, frequently and widely. Every year, millions of people affected and huge property losses by floods were recorded in many parts of the world (Aguirre et al., 2019). Accurate and near-real time flood inundation extraction can offer flood information and help to flood emergency response (Muñoz et al., 2021a).

Manual flood inundation extraction is time-consuming and labor-intensive (Guo and Zhao, 2018). Remote sensing data has short acquisition period and rich band information, is possible for extracting flood inundated areas accurately and quickly (Smith, 1997). With the development of remote sensing technology, multi-spectral (MS) data has shorter update period, more bands and higher resolution, become one of the main resources of flood inundation extraction. However, MS images' inability to penetrate cloud cover makes it difficult to offer accurate ground information in the case of high cloud coverage (Solovey, 2019). Synthetic-aperture radar (SAR) images are not easily affected by external factors such as cloud coverage. However, SAR images always fail to distinguish water from water-like surface (Shen et al., 2019). MS data and SAR data are from different sensors, such that have different advantages for flood inundation extraction. Many studies have combined MS data with SAR data by data fusion methods to obtain more effective features (Konapala et al., 2021).

The data fusion technologies include pixel-level data fusion, feature-level data fusion and decision-level data fusion (Muñoz et al., 2021b). Pixel-level data fusion refers to the direct fusion of the bands from remote sensing images. Pixel-level data fusion is a low-level fusion, which has a strong ability to retain the original information, but it requires higher accuracy on image registration. Therefore, in flood inundation extraction, pixel-level data fusion often exists in the calculation of bands from the same images such as water indices (Benoudjit and Guida, 2019) and HSV transformation (Konapala et al., 2021). Feature-level data fusion is the combination of the features from images. Compared with pixel-level data fusion, feature-level data fusion can extract features from MS data and SAR data flexibly (Gasparovic and Klobucar, 2021).

In recent years, most feature-level data fusion methods using machine learning to combine remote sensing data (Rao et al., 2019). Machine learning algorithms can support the model training with high dimension data. Among the machine learning methods, deep learning with strong learning ability, robustness to noisy data and fault tolerance is increasingly used for flood inundation extraction (Jain et al., 2020). With the continuous improvement of deep learning, the neural networks have evolved from traditional neural network (NN) (Yang et al., n.d.) and fully convolutional network (FCN) (Kang et al., 2018) to UNet and UNet++ (Konapala et al., 2021). Compared with traditional neural network, UNet and UNet++ replace the fully connected layer with a convolution layer, which improves the efficiency of processing for images in large size. Meanwhile, UNet and UNet++ use upsampling and downsampling to integrate low-level features and high-level features (Nemni et al., 2020). The spatial structure helps the networks to extract the features and retain the spatial information. In this way, the pixel segmentation is more accurate.

In feature-level data fusion methods, deep learning models tend to discard some features to optimize the overall accuracy. In

---

* Corresponding author

order to retain the useful features as much as possible, several studies have tried to explore decision-level data fusion methods. Decision-level data fusion is a high level fusion with good fault tolerance and openness (Jia et al., 2000). Traditional decision-level fusion methods include fuzzy logic method (Wendl et al., 2018) and Bayesian method (Bioresita et al., 2019). In recent years, in order to improve the efficiency of data fusion, studies have proposed the concept of master classifier. This method of master classifier firstly uses the most accurate models to classify the images (Lee et al., 2021), and then remains the classification result for the pixels with high confidence, replace the result by the result of joint decision-making with multiple models for the pixels with low confidence. However, most decision-level data fusion methods think less about regional difference and they are difficult to adapt to a large area with complex condition. In order to extract flood inundated areas exactly, this study proposes a data fusion method based on decision tree that can fuse the best results from different models.

2. MATERIALS AND METHODS

2.1 Study area

This study selects flood in Peru, on February 27, 2017 as a case (Figure 1). Piura River is the main source of fresh water, which is essential to the local people. In 2017, heavy rainfall was widespread in Peru due to the Coastal El Niño phenomenon, and it caused major flood in the Piura River basin. Extracting flood inundated areas rapidly and accurately helps emergency response for flood in Peru by offering disaster information in time. Flood inundated areas in Peru from February 2017 to April 2017 are offered by Copernicus EMS. By comparing the flood inundated areas extracted by the decision-level data fusion method with the result from Copernicus EMS, the strengths and weaknesses of the decision-level data fusion method can be analyzed.
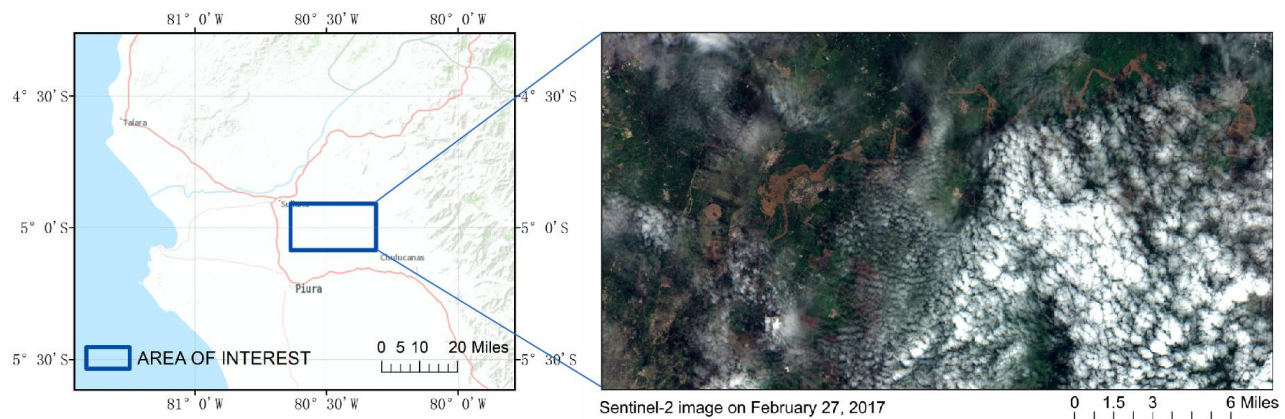

Figure 1. Study area in Peru.

2.2 Data Source

2.2.1   Data Acquisition: This study obtains flood inundated areas from the change of pre-disaster and post-disaster water extent. In order to extract pre-disaster water extent and post-disaster water extent, in this study, Sentinel-2 image on February 16, 2017 and Sentinel-1 image on February 3,2017 are used as pre-disaster data. Sentinel-2 image on February 26, 2017 and Sentinel-1 image on February 27, 2017 are used as post-disaster data (Table 1). After acquire the images, SNAP, a software of remote sensing image processing, is used to pre-process the Sentinel-1 images and the Sentinel-2 images. In order to improve the flood inundation extraction, all the images are 512×512 pixels in size.

Date	Type	Bands
2/3/2017	Sentinel-1	VV,VH
2/16/2017	Sentinel-2	Band1-Band12
2/27/2017	Sentinel-1	VV,VH
2/26/2017	Sentinel-2	Band1-Band12

Table 1. Pre-disaster and post-disaster data for flood in Peru, 2017.

2.2.2   Training Data: In this study, Sen1Floods11 (Bonafilia et al., 2020), which includes 446 sets from 11 flood events around the world, is chosen to train UNet++ models. Every set from Sen1Floods11 contains Sentinel-1 image, Sentinel-2 image and label at 512×512 dimensions. The Sentinel-1 image includes 2 bands, VV band and VH band. The Sentinel-2 image includes 13 bands from Band1 to Band12. The label contains three types of pixels: water, non-water and no data. All the images are projected to WGS 84 at 10 m ground resolution.

2.3 Methods

In this study, UNet++ models are trained by Sen1Floods11 , and the models suitable for cloud-free & non-water area, cloud-free & flood area and cloud area will be selected. The selected models and the pre-processed data in study area are uesed to extract water extents. Then the result from different models is combined by a decision-level data fusion method to obtain the pre-disaster water extent and post-disaster water extent. Finally, the flood inundated areas in study area are obtained by subtracting pre-disaster water extent from post-disaster water extent.
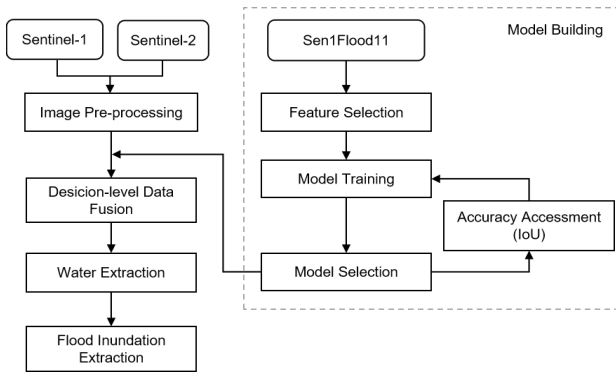
Figure 2. Method of flood inundation extraction.

2.3.1   Feature selection: In order to enable the deep learning model to gain more effective information, besides original bands of Sentinel-1 images and Sentinel-2 images, this study additionally selects a variety of water indices to train models. The selection of water indices is mainly considered about the ground condition of the study area and the image quality of flood in Peru.

First, the study area is located in the western part of South America with an arid climate and a large number of urban areas. It is essential to think about the influence of vegetation and urban buildings when extracting water extent by remote sensing data. Therefore, Normalized Difference Water Index (NDWI) (McFEETERS, 1996), which is sensitive to vegetation is chosen.

$$NDWI = \frac{GREEN - NIR}{GREEN + NIR}, \quad (1)$$

Second, flood is often accompanied by severe weather, and the acquired MS images are prone to the problem of high cloud coverage. Therefore, this study selects the Normalized Difference Multi-band Water Index (NDMBWI) (Deng and Ren, 2021), which can reduce the influence of cloud and shadows on flood inundation extraction.

$$NDMBWI = \frac{3GREEN - BLUE + 2RED - 5NIR}{3GREEN + BLUE + 2RED + 5NIR}, \quad (2)$$

2.3.2   UNet++ Architecture: UNet++ architecture consists of three parts, upsampling, downsamping and skip connection (Zhou et al., 2018). Upsamping is used to extract high-level features. Downsampling is used to extracted Low-level features. Skip connection combines high-level features and low-level features. Compared with UNet, UNet++ has more skip connection processes which make UNet++ architecture more flexible and facilitate the extraction of more features. And because of the nested skip connection, UNet++ can realize deep supervision, which enables model pruning and improves the result.
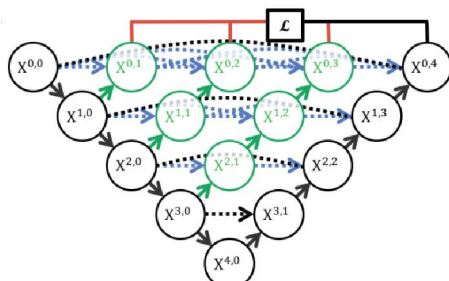

Figure 3. UNet++ architecture(Zhou et al., 2018).

2.3.3   Decision-level data fusion: The decision-level data fusion method in this study improves the overall accuracy of the study area by combining the advantages of different models. Based on the images of the study area, this study divides the whole study area into three parts, cloud-free & non-water area, cloud-free & flood area and cloud area. By evaluating the recall scores (Harman, 2011) of the models in cloud-free & non-water area, cloud-free & flood area and cloud area, this study select the locally optimal models for every area.

Model	Cloud-free & Non-water Area	Cloud-free & Flood Area	Cloud Area
S1	0.96	0.72	**0.81**
S1+Band6	**0.99**	0.47	0.31
S1+Band11	0.98	0.82	0.50
S1+Band12	**0.99**	0.75	0.39
S1+S2+NDMBWI +NDWI	0.98	**0.88**	0.58

Table 2. Recall scores of different models.

The result shows that in cloud area, S1 model performs best. In cloud-free area, S1+S2+NDMBWI+NDWI model has the highest accuracy of water extraction. S1+Band6 model and S1+Band12 model are good at distinguishing non-water pixels. Considering the poor performance of S1+Band6 model in cloud-free & flood area and cloud area, S1+Band12 model is selected to combining with S1 model and S1+S2+NDMBWI+NDWI model.

After selecting the models suitable for cloud-free & non-water area, cloud-free & flood area and cloud area, this study tents to combine the results of models. The specific data fusion process is as follows:

(1) Use S1+Band12 model which is suitable for cloud-free & non-water area to remove most non-water area. The probability of each pixel classified as water is calculated and the pixels with probability lower than k1 are defined as non-water and the pixels with probability higher than k1 are defined as unknown.

(2) Use S1+S2+NDMBWI+NDWI model which is suitable for cloud-free & non-water area to extract the water extent in the unknown region from the first step. The pixels with probability higher than k2 are defined as the water and the pixels with probability lower than k2 are defined as unknown.

(3) Use S1 model which is suitable for cloud area to extract the water extent in the unknown region from the second step.
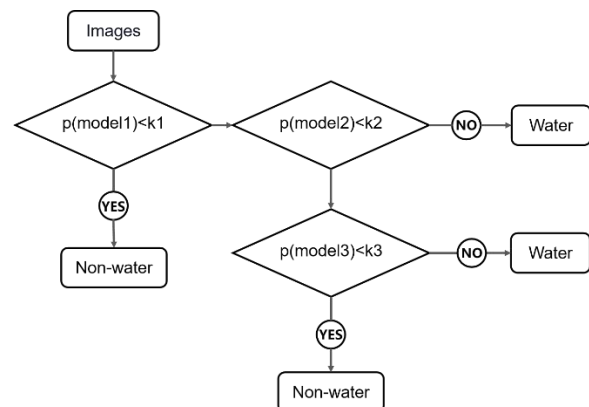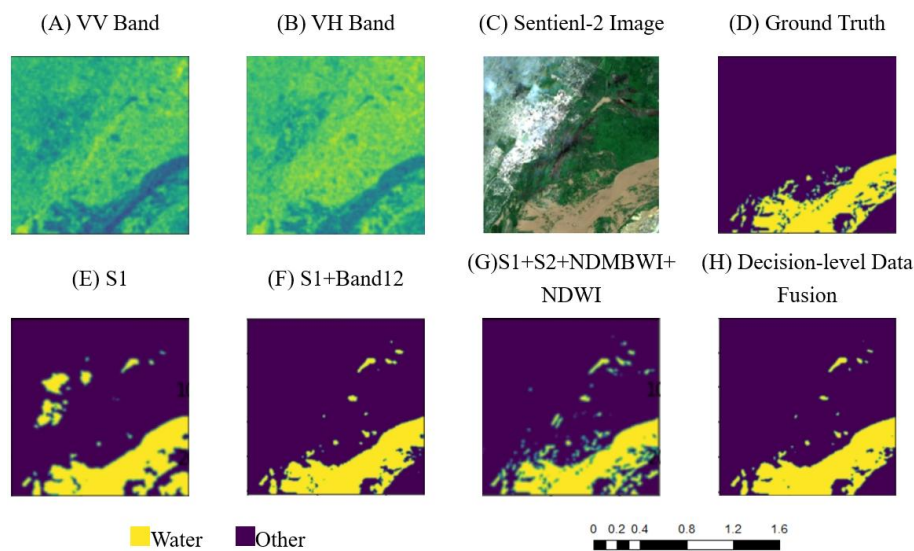

Figure 4. Decision-level data fusion method.

Before implementing the decision-level data fusion method, three probability thresholds need to be determined. Firstly, the recall scores of S1+Band12 model when extracting non-water area with different probability threshold (k1) are calculated. When k1 is 0.4, S1 model has higher recall and less classification error. Secondly, after removing non-water areas by S1+Band12 model, the recall scores of S1+S2+NDMBWI+NDWI model when extracting water extent with different probability thresholds (k2) are calculated. When k2 is 0.95, S1+S2+NDMBWI+NDWI model has the best result. Finally, the loUs of the S1 model are calculated in the remaining area. When the probability threshold (k3) is 0.5, S1 model gets the highest IoU.
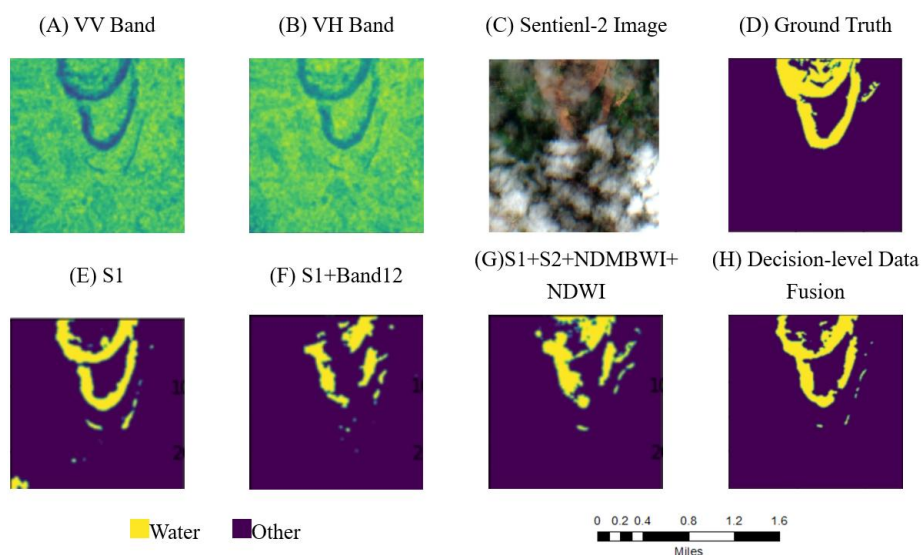
2.3.4 Precision evaluation criteria: By the deep learning model, the image can be divided into two parts: water and non-water, from which true positive (TP), true negative (TN), false positive (FP) and false negative (FN) can be calculated. By calculating the above metrics, precision and recall can be obtained to evaluate the effectiveness of the model. However, the precision only reflects the accuracy of the water region extracted by the model while the recall only reflects the difference between the water classified by the model and the real water region. Both of them can reflect the extraction effect of models but each has limitations, so this study uses Intersection over Union (IoU) (Cai and Vasconcelos, 2018) as the criterion to evaluate models. IoU considers the influence of the water that is misclassified and the water that fails to be extracted. The specific formula is as follows:

$$IOU = TP/(TP + TN + FP), \qquad (3)$$

Figure 5. Results of data fusion in cloud-free area.

(A) VV Band   (B) VH Band   (C) Sentienl-2 Image   (D) Ground Truth

(E) S1   (F) S1+Band12   (G)S1+S2+NDMBWI+NDWI   (H) Decision-level Data Fusion

Water   Other

Figure 6. Results of data fusion in cloud area.

(A) VV Band   (B) VH Band   (C) Sentienl-2 Image   (D) Ground Truth

(E) S1   (F) S1+Band12   (G)S1+S2+NDMBWI+NDWI   (H) Decision-level Data Fusion

Water   Other

3. RESULTS

3.1 Decision-level data fusion

In order to analyze the effect of the decision-level data fusion method, this study use IoU to compares the decision-level data fusion method with the sub models. Table 3 presents the IoUs. The results show that the IoU increases after decision-level data fusion, which means the decision-level data fusion method improves the water extraction in the whole study area.

Model	IoU
S1	0.56
S1+Band12	0.57
S1+S2+NDMBWI+NDWI	0.68
Fusion	0.69

Table 3. IoUs before and after decision-level data fusion.

Besides accuracy assessment, the maps of water extraction are also important to evaluating the decision-level data fusion method. In order to present more characteristics of the decision-level data fusion method, the maps of water extraction should be compared in cloud-free area and cloudarea. Figure 5

presents the extraction in cloud-free area and Figure 6 presents the extraction in cloud area. According to the results, the water extent extracted by S1 model is generally consistent with the real water extent in cloud area, while it includes many water-like surfaces. S1+Band12 model has a better performance in removing non-water area, but it can't extract water extent accurately. S1+S2+NDMBWI+NDWI model is good at water extraction in cloud-free area, but it failed to extract water extent completely in cloud area.

Compared with the results of the sub models, the decision-level data fusion method effectively reduces the influence of shadow on water extraction. Meanwhile, in cloud area, the decision-level data fusion method can produce a more complete map of water.

3.2 Flood inundation extraction in study area

In this study, we use the method of subtracting the pre-disaster water extent from the post-disaster water extent to obtain the flood inundated areas. Based on the method, this study collects pre-disaster and post-disaster remote sensing images for flood in Peru and extracts the pre-disaster water extent and post-disaster water extent using a decision-level data fusion method. The flood inundated area in study area on February 27, 2017 is about 12809591 m^2.
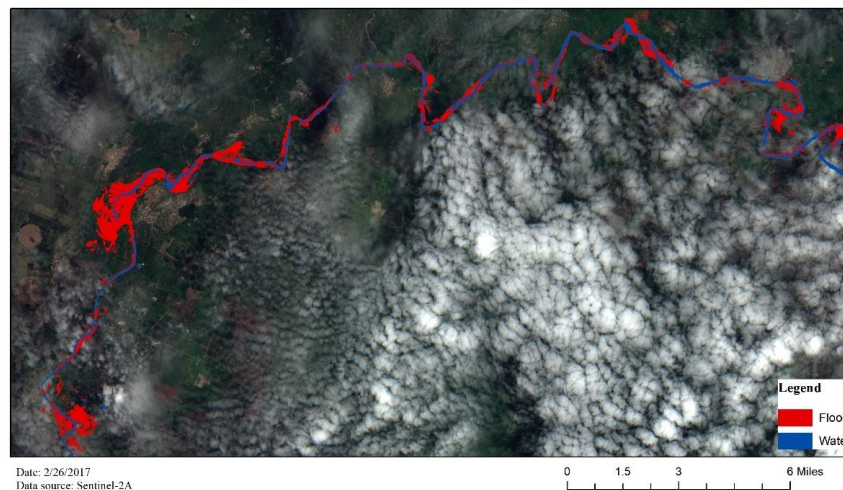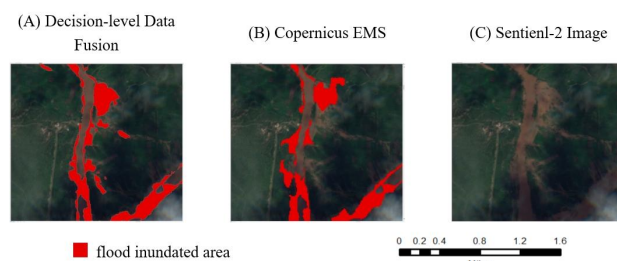

Figure 7. Flood inundated areas in study area on February 27, 2017 extracted by decision-level data fusion method.
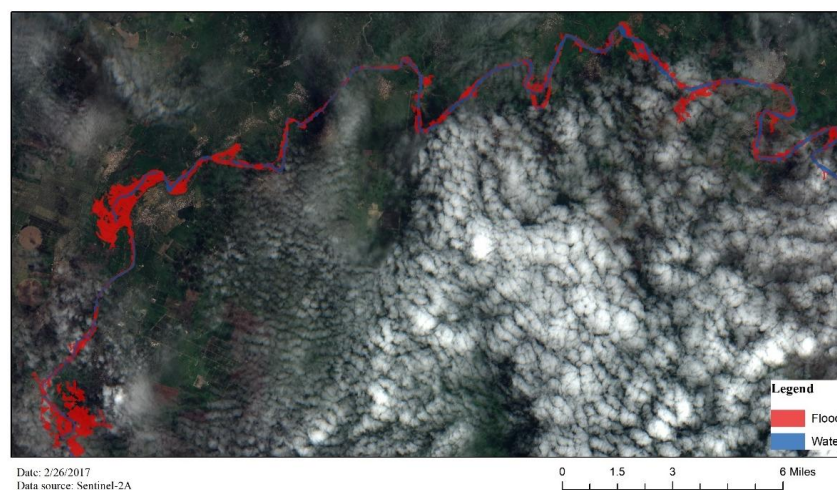
Figure 8. Flood inundated areas in study area on February 27,2017 from Copernicus EMS.

To analyze the actual effect of the decision-level data fusion method deeply, we refer to the result of the flood in Peru, 2017 from Copernicus EMS and compare the result with the flood inundated areas extracted by our decision-level data fusion method.

To be more convenient, the manually labeled flood inundated areas in study area on February 27, 2017 is used as the true value. The result of decision-level data fusion method and the result from Copernicus EMS are compared by the IoU of flood inundation extraction. The result shows that the IoU of the flood inundated areas from Copernicus EMS is 0.44 and the IoU of the decision level data fusion method is 0.50. In terms of details, the decision-level data fusion method incorporates features such as NDMBWI, and thus has advantages in distinguishing water from shadows. Meanwhile, the decision-level data fusion method combines the advantages of multiple models, so, it has better extraction at flooding edge areas and the areas with more fragmented flooding distribution.

(A) Decision-level Data Fusion   (B) Copernicus EMS   (C) Sentienl-2 Image

■ flood inundated area

Figure 9. Flood inundated areas in study area (partial) on February 27, 2017.

4. DISCUSSIONS

In this study, we propose a decision-level data fusion method based on decision tree. Before constructing the decision-level data fusion method, different models are needed.

In the process of constructing models, we try to combine multiple features. Among the features, bands of Sentinel-1 offer the texture information, bands of Sentinel-2 offer spectral information, NDWI helps to distinguish water from vegetation, NDMBWI reduces the influence of cloud and shadows on water extraction. All the features contribute to water extraction. However, the model with highest accuracy which combine all the features we selected, is still difficult to distinguish water from bare soil. Through the analysis of the water in study area, we find that there is much sediment in the water. It makes the water during flood more similar to bare soil than normal water. In this study, the features we selected lack of the ability to distinguish flood water from bare soil, which may be one of the reasons why our model fails to extract water extent effectively.

Besides the selection of features, the training set has a great impact on model training. In the result, the IoU of the models in training set are always higher than the IoU in study area. It means the models are more suitable for the training set. In this study, we select Sen1Flood11 as training set, which lacks data with high cloud coverage. It leads to the models being more applicable to the area with less cloud.

After model training, this study construct data fusion method by decision tree. The result shows that our decision-level data fusion method improve the IoU of water extraction. However, the improvement is not significant. There are two main reasons

lead to the phenomenon. First, the input variables of data fusion method and S1+S2+NDWI+NDMBWI model are the same, which means our decision-level data fusion method does not learn more features. Second, this study pays more attention to the extraction effect in cloud area. In order to avoid the cloud area being classified as non-water in the first step of the decision tree, we think more about the extraction in cloud area than the accuracy in cloud-free area during the selection of threshold, which may influence the water extraction in cloud-free area.

Of course, in addition to some problems in model training and construction of data fusion method, the study area data itself has a large impact on the water extraction in study area. In this study, the Sentinel-1 and Sentinel-2 images of study area are not at the same time such as the post-disaster Sentinel-1 image imaged on February 27, 2017 and the post-disaster Sentinel-2 image imaged on February 26, 2017. During the period of flooding, the extent of water changes rapidly and there are more obvious differences between the water extent on February 26, 2017 and February 27, 2017 in some sections of the river.

5. CONCLUSIONS

In this study we combine different models to construct a decision-level data fusion method. By comparing the results before and after fusion, we found that the decision-level data fusion method successfully reduces the influence of clouds and shadows on water extraction by utilizing the features from NDWI, NDMBWI and Sentinel-1/2 original bands effectively. Then we use the decision-level data fusion method to extract pre-disaster water extent and post-disaster water extent, which can be used to obtain the flood inundated areas in Peru on February 27, 2017. By comparing the flood inundated areas we extracted with the result offered by Copernicus EMS, it proves that the decision-level data fusion method has advantage in study area. Although the decision-level data fusion method has obtained excellent result, there is still plenty of room to optimize the selection of water indices and the construction of decision-level data fusion methods. First, this study does not take the difference between flood and general water into account, so it is expected to choose more suitable indices for the model in the next stage of exploration. Second, in the process of constructing the decision-level data fusion method, the selection of thresholds is too subjective and we can try to use an efficient and explanatory way to select the thresholds automatically.

REFERENCES

Aguirre, J., De La Torre Ugarte, D., Bazo, J., Quequezana, P., Collado, M., 2019. Evaluation of Early Action Mechanisms in Peru Regarding Preparedness for El Niño. *Int J Disaster Risk Sci* 10, 493–510. https://doi.org/10.1007/s13753-019-00245-x

Benoudjit, A., Guida, R., 2019. A Novel Fully Automated Mapping of the Flood Extent on SAR Images Using a

Supervised Classifier. *Remote Sensing* 11, 779. https://doi.org/10.3390/rs11070779

Bioresita, F., Puissant, A., Stumpf, A., Malet, J.-P., 2019. Fusion of Sentinel-1 and Sentinel-2 image time series for permanent and temporary surface water mapping. *International Journal of Remote Sensing* 40, 9026–9049. https://doi.org/10.1080/01431161.2019.1624869

Bonafilia, D., Tellman, B., Anderson, T., Issenberg, E., 2020. Sen1Floods11: A Georeferenced Dataset to Train and Test Deep Learning Flood Algorithms for Sentinel-1. pp. 210–211.

Cai, Z., Vasconcelos, N., 2018. Cascade R-CNN: Delving Into High Quality Object Detection, in: 2018 IEEE/CVF Conference on Computer Vision and Pattern Recognition. pp. 6154–6162. https://doi.org/10.1109/CVPR.2018.00644

Deng, K., Ren, C., 2021. Water Extraction Model of Multispectral Optical Remote Sensing Image. *Acta Geodetica et Cartographica Sinica* 50, 1370–1379.

Feyisa, G.L., Meilby, H., Fensholt, R., Proud, S.R., 2014. Automated Water Extraction Index: A new technique for surface water mapping using Landsat imagery. *Remote Sensing of Environment* 140, 23–35. https://doi.org/10.1016/j.rse.2013.08.029

Guo, X., Zhao, Y., 2018. Flood inundation Monitoring in Ningxiang of Hunan Province based on Sentinel-1 SAR. *Remote Sensing Technology and Application* 33, 646–656.
Gasparovic, M., Klobucar, D., 2021. Mapping Floods in Lowland Forest Using Sentinel-1 and Sentinel-2 Data and an Object-Based Approach. *Forests* 12, 553. https://doi.org/10.3390/f12050553

Harman, D., 2011. Information Retrieval Evaluation. Synthesis Lectures on Information Concepts, Retrieval, and Services 3, 1–119.
https://doi.org/10.2200/S00368ED1V01Y201105ICR019

Jain, P., Schoen-Phelan, B., Ross, R., 2020. Automatic flood detection in SentineI-2 images using deep convolutional neural networks, in: Proceedings of the 35th Annual ACM Symposium on Applied Computing. ACM, Brno Czech Republic, pp. 617–623. https://doi.org/10.1145/3341105.3374023

Jia, Y., Lee, D., Sun, J., 2000. Data Fusion Techniques for Multisources Remotely Sensed Imagery. *Remote Sensing Technology and Application* 41–44.

Kang, W., Xiang, Y., Wang, F., Wan, L., You, H., 2018. Flood Detection in Gaofen-3 SAR Images via Fully Convolutional Networks. *Sensors* 18, 2915. https://doi.org/10.3390/s18092915

Konapala, G., Kumar, S.V., Khalique Ahmad, S., 2021. Exploring Sentinel-1 and Sentinel-2 diversity for flood inundation mapping using deep learning. *ISPRS Journal of Photogrammetry and Remote Sensing* 180, 163–173. https://doi.org/10.1016/j.isprsjprs.2021.08.016

Lee, H., Gao, X., Tang, M., 2021. Land Cover Classification for SPOT-6 Image from Decision Fusion Method . *Journal of Geo-information Science* 23, 928–937.

McFEETERS, S.K., 1996. The use of the Normalized Difference Water Index (NDWI) in the delineation of open water features. *International Journal of Remote Sensing* 17, 1425–1432. https://doi.org/10.1080/01431169608948714

Muñoz, D.F., Muñoz, P., Alipour, A., Moftakhari, H., Moradkhani, H., Mortazavi, B., 2021a. Fusing Multisource Data to Estimate the Effects of Urbanization, Sea Level Rise, and Hurricane Impacts on Long-Term Wetland Change Dynamics. *IEEE Journal of Selected Topics in Applied Earth Observations and Remote Sensing* 14, 1768–1782. https://doi.org/10.1109/JSTARS.2020.3048724

Muñoz, D.F., Muñoz, P., Moftakhari, H., Moradkhani, H., 2021b. From local to regional compound flood mapping with deep learning and data fusion techniques. *Science of The Total Environment* 782, 146927. https://doi.org/10.1016/j.scitotenv.2021.146927

Nemni, E., Bullock, J., Belabbes, S., Bromley, L., 2020. Fully Convolutional Neural Network for Rapid Flood Segmentation in Synthetic Aperture Radar Imagery. *Remote Sensing* 12, 2532. https://doi.org/10.3390/rs12162532

Rao, P., Jiang, W., Wang, X., Chen, K., 2019. Flood disaster analysis based on MODIS data:Taking the flood in dongting lake area in 2017 as an example. *Journal of Catastrophology* 34, 203–207.

Shen, X., Wang, D., Mao, K., Anagnostou, E., Hong, Y., 2019. Inundation Extent Mapping by Synthetic Aperture Radar: A Review. *Remote Sensing* 11, 879. https://doi.org/10.3390/rs11070879

Smith, L.C., 1997. Satellite remote sensing of river inundation area, stage, and discharge: a review. *Hydrological Processes* 11, 1427–1439. https://doi.org/10.1002/(SICI)1099-1085(199708)11:10<1427::AID-HYP473>3.0.CO;2-S

Solovey, T., 2019. An analysis of flooding coverage using remote sensing within the context of risk assessment. *Geologos* 25, 241–248. https://doi.org/10.2478/logos-2019-0026

Wang, D., Wang, S., Huang, C., 2019. Comparison of Sentinel-2 imagery with Landsat8 imagery for surface water extraction using four common water indexes. *Remote Sensing for Land & Resources* 31, 157–165.

Wendl, C., Bris, A.L., Chehata, N., Puissant, A., Postadjian, T., 2018. Decision Fusion of Spot6 And Multitemporal Sentinel2 Images For Urban Area Detection, in: IGARSS 2018 - 2018 IEEE International Geoscience and Remote Sensing Symposium. pp. 1734–1737. https://doi.org/10.1109/IGARSS.2018.8517476

Yang, L., Tian, S., Yu, L., Ye, F., Qian, J., Qian, Y., n.d. DEEP LEARNING FOR EXTRACTING WATER BODY FROM LANDSAT IMAGERY 17.

Zhou, Z., Rahman Siddiquee, M.M., Tajbakhsh, N., Liang, J., 2018. UNet++: A Nested U-Net Architecture for Medical Image Segmentation, in: Stoyanov, D., Taylor, Z., Carneiro, G., Syeda-Mahmood, T., Martel, A., Maier-Hein, L., Tavares, J.M.R.S., Bradley, A., Papa, J.P., Belagiannis, V., Nascimento, J.C., Lu, Z., Conjeti, S., Moradi, M., Greenspan, H., Madabhushi, A. (Eds.), Deep Learning in Medical Image Analysis and Multimodal Learning for Clinical Decision

Support, Lecture Notes in Computer Science. Springer International Publishing, Cham, pp. 3–11. https://doi.org/10.1007/978-3-030-00889-5_1